PROCEEDINGS A

rspa.royalsocietypublishing.org

Research

Cite this article: Kevrekidis PG, Pelinovsky DE. 2017 On the characterization of vortex configurations in the steady rotating Bose–Einstein condensates. *Proc. R. Soc. A* **473**: 20170602.
http://dx.doi.org/10.1098/rspa.2017.0602

Received: 5 September 2017
Accepted: 10 November 2017

Subject Areas:
differential equations, applied mathematics, low temperature physics

Keywords:
Gross–Pitaevskii equation, rotating vortices, harmonic potentials, bifurcations, stability, energy minimization

Author for correspondence:
D. E. Pelinovsky
e-mail: dmpeli@math.mcmaster.ca

On the characterization of vortex configurations in the steady rotating Bose–Einstein condensates

P. G. Kevrekidis[1] and D. E. Pelinovsky[2,3]

[1]Department of Mathematics and Statistics, University of Massachusetts, Amherst, MA 01003, USA
[2]Department of Mathematics and Statistics, McMaster University, Hamilton, Ontario, Canada L8S 4K1
[3]Department of Applied Mathematics, Nizhny Novgorod State Technical University, 24 Minin street, 603950 Nizhny Novgorod, Russia

DEP, 0000-0001-5812-440X

Motivated by experiments in atomic Bose–Einstein condensates (BECs), we compare predictions of a system of ordinary differential equations (ODEs) for dynamics of one and two individual vortices in the rotating BECs with those of the Gross–Pitaevskii mean-field model written as a partial differential equation (PDE). In particular, we characterize orbitally stable vortex configurations in a symmetric harmonic trap due to a cubic repulsive interaction and a steady rotation. The ODE system is analysed in detail and the PDE model is approximated numerically. Good agreement between the two models is established in the semi-classical (Thomas–Fermi) limit that corresponds to the BECs at large values of the chemical potential.

1. Introduction

Our principal interest in the present work focuses on the dynamics of vortex excitations in atomic Bose–Einstein condensates (BECs) [1] and their description with the Gross–Pitaevskii (GP) equation [2]. Early works on the subject, summarized in the review [3], as well as more recent experimental work such as in [4], highlight the ongoing interest towards a quantitative characterization of vortex configurations of minimal energy by means of low-dimensional models involving ordinary differential equations (ODEs). This is an

THE ROYAL SOCIETY PUBLISHING

endeavour that was initiated in the pioneering work of Castin & Dum [5] and has now matured to the point that it can be used to understand the dynamics of such systems in experimental time series such as those of Navarro *et al*. [4] (see also the relevant analysis of Zampetaki *et al*. [6]). Our aim in the present work is to characterize orbitally stable vortex configurations among steadily rotating solutions to the GP equation.

More specifically, we address the GP equation for a BEC in two dimensions with a cubic repulsive interaction and a symmetric harmonic trap. This model can be written in the normalized form

$$\mathrm{i}\varepsilon u_t = -\varepsilon^2 \Delta u + (|x|^2 + |u|^2 - 1)u, \tag{1.1}$$

where $\Delta = \partial_x^2 + \partial_y^2$ and $|x|^2 = x^2 + y^2$. By means of the transformation $u = \sqrt{\varepsilon}\tilde{u}$ and $x = \sqrt{\varepsilon}\tilde{x}$, the model can be rewritten in the form

$$\mathrm{i}\tilde{u}_t = -\tilde{\Delta}\tilde{u} + (|\tilde{x}|^2 + |\tilde{u}|^2 - \mu)\tilde{u}, \tag{1.2}$$

where $\mu = \varepsilon^{-1}$ is the chemical potential. Naturally, the regime where ε is a small parameter corresponds to the regime of the large chemical potential μ. In this semi-classical (Thomas–Fermi) limit $\varepsilon \to 0$, vortices behave qualitatively as individual particles with no internal structure [2].

The associated energy of the GP equation (1.1) is given by

$$E(u) = \iint_{\mathbb{R}^2} \left[\varepsilon^2 |\nabla u|^2 + (|x|^2 - 1)|u|^2 + \frac{1}{2}|u|^4 \right] \mathrm{d}x\, \mathrm{d}y. \tag{1.3}$$

Time-independent solutions to the GP equation (1.1) are critical points of the energy (1.3).

Among the stationary solutions of the GP equation (1.1), there is a *ground state* (global minimizer) of the energy $E(u)$ subject to a fixed value of mass $Q(u) = \|u\|^2$. The ground state is a radially symmetric, real, positive stationary solution with a fast decay to zero at infinity. Properties of the ground state in the semi-classical limit $\varepsilon \to 0$ were studied in [7,8]. On the other hand, vortices are complex-valued stationary solutions with a non-zero winding number along a circle of large radius centred at the origin. Vortices are less energetically favourable, as they are saddle points of the energy $E(u)$ subject to a fixed value of mass $Q(u)$. However, when the BEC is rotated with a constant angular frequency ω, it was realized long ago [3] that the vortex configurations may become energetically favourable depending on the frequency ω due to the contribution of the z-component of the angular momentum in the total energy.

From a mathematical perspective, Ignat & Millot [8,9] confirmed that the vortex of charge one near the centre of symmetry is a global minimizer of total energy for a frequency ω above a first critical value ω_1^*. Seiringer [10] proved that a vortex configuration with charge m becomes energetically favourable to a vortex configuration with charge $(m-1)$ for a frequency ω above the mth critical value $\omega_m^* > \omega_{m-1}^*$ and that radially symmetric vortices with charge $m \geq 2$ cannot be minimizers of total energy. It is natural to conjecture that the vortex configuration of charge m with the minimal total energy consists of m individual vortices of charge one, which are placed near the centre of symmetry. The location of individual vortices has not been rigorously discussed in the previous works [8–10], although it has been the subject of many studies (see relevant examples in [4–6]).

For the vortex of charge one, it was shown by using variational approximations [5] and bifurcation methods [11] that the radially symmetric vortex becomes a local minimizer of total energy past the threshold value ω_1 of the rotation frequency ω, where $\omega_1 \leq \omega_1^*$. In addition to the radially symmetric vortex, which exists for all values of ω, there exists another branch of the asymmetric vortex solutions above the threshold value, for $\omega > \omega_1$. The branch is represented by a vortex of charge one displaced from the centre of the rotating symmetric trap. Although the asymmetric vortex is not a local energy minimizer, it is nevertheless a constrained energy minimizer subject to the constraint eliminating the rotational invariance of the asymmetric vortex. Consequently, both radially symmetric and asymmetric vortices are orbitally stable in the time evolution of the GP equation (1.1) for the rotation frequency ω slightly above the threshold value ω_1 [11].

Stability of equilibrium configurations of several vortices of charge one in rotating harmonic traps was investigated numerically in [12–17] (although a number of these studies have involved also vortices of opposite charge). The numerical results were compared with the predictions given by the finite-dimensional ODE system for dynamics of individual vortices [4,6,18,19]. The relevant dynamics even for systems of two vortices remain a topic of active theoretical investigation [20], including the study of a vortex pair evolving in an inhomogeneous background [21] and the examination of instability of dark solitons and vortex pairs without the external potential [22].

In the case of two vortices, the equilibrium configuration with the minimal total energy emerges again above the threshold value ω_2 for the rotation frequency ω, where $\omega_2 > \omega_1$. The relevant configuration consists of two vortices of charge one being located symmetrically with respect to the centre of the harmonic trap. However, the symmetric vortex pair is stable only for small distances from the centre and it loses stability for larger distances [4]. Once it becomes unstable, another asymmetric configuration involving two vortices bifurcates with one vortex being at a smaller-than-critical distance from the centre and the other vortex being at a larger-than-critical distance from the centre. The asymmetric pair is stable in numerical simulations and coexists for rotating frequencies above the value ω_2 with the stable symmetric vortex pair located at the smaller-than-critical distances [4,6].

In this work, we revisit the ODE models for configurations of two vortices of charge one in the semi-classical limit $\varepsilon \to 0$. We will connect the details of bifurcations observed in [4,6] with the stability properties of vortices due to their energy minimization properties. Compared with our previous work [16], we will incorporate an additional term in the expansion of the vortex kinetic energy, which is responsible for the nonlinear dependence of the vortex precession frequency on the vortex distance from the origin. This improvement corresponds exactly to the theory used in the physics literature; see, e.g. the review [3]. The additional term in the total energy derived in appendix A allows us to give all details on the characterization of energy minimizers and orbital stability in the case of one and two vortices of charge one.

In particular, we recover the conclusions obtained from the bifurcation theory in [11] that the symmetric vortex of charge one is an energy minimizer for $\omega > \omega_1$ and that the asymmetric vortex of charge one is a constrained energy minimizer for $\omega > \omega_1$. Both vortex configurations are stable in the time evolution of the GP equation (1.1).

We also show from the ODE model that the symmetric pair of two vortices of charge one is an energy minimizer for $\omega > \omega_2$, whereas the asymmetric pair is a local constrained minimizer of energy for $\omega > \omega_2$. In this case too, for $\omega > \omega_2$, both vortex configurations are stable in the time evolution of the GP equation (1.1). A fold bifurcation of the symmetric vortex pair occurs at a frequency ω smaller than ω_2 with both branches of symmetric vortex pairs being unstable near the fold bifurcation. This instability is due to the symmetric vortex pairs for $\omega < \omega_2$ being saddle points of total energy even in the presence of the constraint eliminating rotational invariance of the vortex configuration.

Although the ODE model is not rigorously justified in the context of the GP equation (1.1), we confirm numerically that the predictions of the ODE model hold exactly as qualitatively predicted within the partial differential equation (PDE) model in the semi-classical limit $\varepsilon \to 0$.

Next, we mention a number of recent studies on vortex configurations of the GP equation (1.1) in the case of steady rotation. In the small-amplitude limit, when the reduced models are derived by using the decompositions over the Hermite–Gauss eigenfunctions of the quantum harmonic oscillator, a classification of localized (soliton and vortex) solutions from the triple eigenvalue was constructed in [23]. Bifurcations of radially symmetric vortices with charge $m \in \mathbb{N}$ and dipole solutions were studied in [24] with the help of the equivariant degree theory. Bifurcations of multi-vortex configurations in the parameter continuation with respect to the rotation frequency ω were considered in [25]. Existence and stability of stationary states were analysed in [26] with the resonant normal forms. Some exact solutions of the resonant normal forms were reported recently in [27]. Vortex dipoles were studied with the normal form equations in the presence of an anisotropic trap in [28].

Compared with the recent works developed in the small-amplitude limit, our results here are expected to be valid only in the semi-classical limit $\varepsilon \to 0$, i.e. for large chemical potential μ rather than for values of the chemical potential in the vicinity of the linear limit. As a result, our conclusions are slightly different from those that hold in the small-amplitude limit.

In [25], it was shown that the asymmetric pair of two vortices of charge one bifurcates from the symmetric vortex of charge two and that this vortex pair shares the instability of the symmetric vortex of charge two in the small-amplitude limit. This instability is due to the fact that the vortex pair is a saddle point of total energy above the bifurcation threshold in the small-amplitude limit. It is presently an open question to explore how this bifurcation diagram deforms when the chemical potential is changed from the small-amplitude limit to the semi-classical (Thomas–Fermi) limit.

Recent computational explorations of the stationary configurations of vortices have been performed with several alternative numerical methods [29–31]. A principal direction of attention is drawn to the global minimizers of total energy in the case of fast rotation, when the computational domain is filled with the triangular lattice of vortices [30,31]. Dissipation is also included in order to regularize the computational algorithms [31] or to enable convergence in the case of ground states [30]. Although the ODE models are very useful to characterize one and two vortices, it becomes cumbersome to characterize three and more vortices, and naturally the complexity increases significantly in the case of larger clusters and especially for triangular vortex lattices. Hence, such cases will not be addressed, although the tools utilized here can, in principle, be generalized therein.

Our work paves the way for numerous developments in the future. Constructing multi-vortex configurations and lattices of such vortices in a systematic way at the ODE level is definitely a challenging problem for better understanding of dynamics in the GP equation. Another important direction of recent explorations in BECs has involved the phenomenology of vortex lines and vortex rings in the space of three dimensions [2]. The consideration of similar notions of effective dynamical systems describing, e.g. multiple vortex rings is a topic under active investigation and one that bears some nontrivial challenges from the ODE theory [32].

Finally, we mention that vortex ODE theory has been found very useful to characterize travelling waves in the defocusing nonlinear Schrödinger equation in the absence of rotation and the harmonic potential [33,34] (see also the recent work [35]).

The remainder of this paper is organized as follows. Section 2 reports predictions of the ODE model for a single vortex of charge one. Section 3 is devoted to analysis of the ODE model for a pair of vortices of charge one. Section 4 gives numerical results for the vortex pairs. Section 5 presents our conclusion. Appendix A contains the derivation of the additional term in the expansion of the vortex kinetic energy.

2. Reduced energy for a single vortex of charge one

A single vortex of charge one shifted from the centre of the harmonic potential behaves like a particle with the corresponding kinetic and potential energy [2]. The asymptotic expansions of kinetic and potential energy were derived in [16] by using a formal Rayleigh–Ritz method and analysis of resulting integrals in the semiclassical limit of $\varepsilon \to 0$. By Lemmas 1 and 2 in [16], a single vortex of charge one placed at the point $(x_0, y_0) \in \mathbb{R}^2$ has kinetic K and potential P energies given by

$$K(x_0, y_0) = \tfrac{1}{2}\varepsilon(x_0\dot{y}_0 - y_0\dot{x}_0)\,[1 + \mathcal{O}(\varepsilon + x_0^2 + y_0^2)] \tag{2.1}$$

and

$$P(x_0, y_0) = \tfrac{1}{2}\varepsilon\omega_0(\varepsilon)(x_0^2 + y_0^2)\,[1 + \mathcal{O}(\varepsilon^{1/3} + x_0^2 + y_0^2)], \tag{2.2}$$

where $\omega_0(\varepsilon) = -2\varepsilon\log(\varepsilon) + \mathcal{O}(1)$ as $\varepsilon \to 0$ and we have divided all expressions by 2π compared with [16]. Let us truncate the expansions (2.1) and (2.2) by the leading-order terms and obtain the

Euler–Lagrange equations for the Lagrangian $L(x_0, y_0) = K(x_0, y_0) - P(x_0, y_0)$. The corresponding linear system divided by ε is

$$\left.\begin{aligned} \dot{y}_0 - \omega_0(\varepsilon) x_0 = 0, \\ -\dot{x}_0 - \omega_0(\varepsilon) y_0 = 0, \end{aligned}\right\} \quad \Rightarrow \quad \ddot{x}_0 + \omega_0(\varepsilon)^2 x_0 = 0 \tag{2.3}$$

and it exhibits harmonic oscillators with the frequency $\omega_0(\varepsilon)$. This frequency was compared in [16] with the smallest eigenvalue in the spectral stability problem for the single vortex of charge one, a good agreement was found as the asymptotic limit $\varepsilon \to 0$ was approached.

It was suggested heuristically in [3] (see also [18,19]) that the frequency of vortex precession depends on the displacement a of a single vortex of charge one from the centre of the harmonic potential by the following law:

$$\omega(a) = \frac{\omega_0(\varepsilon)}{1 - a^2}, \quad a \in (0, 1), \tag{2.4}$$

so that $\omega(a) > \omega_0(\varepsilon)$. This law is in agreement with the bifurcation theory for a single asymmetric vortex in the stationary GP equation [11], where a new branch of stationary vortex solutions displaced from the centre of the harmonic potential by the distance $a \sim (\omega - \omega_0(\varepsilon))^{1/2}$ was shown to exist for $\omega \gtrsim \omega_0(\varepsilon)$.

The empirical law (2.4) and the bifurcation of asymmetric vortices for $\omega \gtrsim \omega_0(\varepsilon)$ can be explained by the extension of the kinetic energy given by (2.1) at the same order of ε but to the higher order in $x_0^2 + y_0^2$. We show in appendix A that the kinetic energy $K(x_0, y_0)$ can be further expanded as follows:

$$K(x_0, y_0) = \tfrac{1}{2}\varepsilon(x_0 \dot{y}_0 - y_0 \dot{x}_0)[1 - \tfrac{1}{2}(x_0^2 + y_0^2) + \mathcal{O}(\varepsilon + x_0^4 + y_0^4)]. \tag{2.5}$$

In the reference frame rotating with the angular frequency ω, we can use the polar coordinates

$$x_0 = \xi_0 \cos(\omega t) - \eta_0 \sin(\omega t) \quad \text{and} \quad y_0 = \xi_0 \sin(\omega t) + \eta_0 \cos(\omega t) \tag{2.6}$$

and rewrite the truncated kinetic and potential energies as follows:

$$K(\xi_0, \eta_0) = \tfrac{1}{2}\varepsilon(\xi_0 \dot{\eta}_0 - \dot{\xi}_0 \eta_0) + \tfrac{1}{2}\varepsilon\omega(\xi_0^2 + \eta_0^2)[1 - \tfrac{1}{2}(\xi_0^2 + \eta_0^2)],$$

and

$$P(\xi_0, \eta_0) = \tfrac{1}{2}\varepsilon\omega_0(\varepsilon)(\xi_0^2 + \eta_0^2),$$

where the nonlinear correction for the quadratic term $(\xi_0 \dot{\eta}_0 - \dot{\xi}_0 \eta_0)$ in $K(\xi_0, \eta_0)$ is dropped to simplify the time evolution of the ODE system. In the remainder of this section, we review the existence and stability results for the single vortex of charge one within the ODE theory.

(a) Existence of steadily rotating vortices

Steadily rotating vortices are critical points of the action functional

$$E_1(\xi_0, \eta_0) = \tfrac{1}{2}\varepsilon\omega(\xi_0^2 + \eta_0^2)[1 - \tfrac{1}{2}(\xi_0^2 + \eta_0^2)] - \tfrac{1}{2}\varepsilon\omega_0(\varepsilon)(\xi_0^2 + \eta_0^2). \tag{2.7}$$

Thanks to the rotational invariance, one can place the steadily rotating vortex to the point $(\xi_0, \eta_0) = (a, 0)$. The Euler–Lagrange equation for $E_1(a, 0)$ yields

$$\frac{\mathrm{d}}{\mathrm{d}a} E_1(a, 0) = \varepsilon\omega a(1 - a^2) - \varepsilon\omega_0(\varepsilon) a = 0.$$

Two solutions exist: one with $a = 0$ for every ω and the other one with $a \in (0, 1)$ for $\omega(a)$ given by the dependence (2.4). The symmetric vortex with $a = 0$ exists for every ω, whereas the asymmetric vortex with the displacement $a > 0$ exists for $\omega > \omega_0(\varepsilon)$.

(b) Variational characterization of the individual vortices

Extremal properties of the two critical points of $E_1(\xi_0, \eta_0)$ are studied from the Hessian matrix $E_1''(a, 0)$. This is a diagonal matrix with the diagonal entries:

$$\partial_{\xi_0}^2 E_1(a,0) = \varepsilon\omega(1-3a^2) - \varepsilon\omega_0(\varepsilon) \quad \text{and} \quad \partial_{\eta_0}^2 E_1(a,0) = \varepsilon\omega(1-a^2) - \varepsilon\omega_0(\varepsilon).$$

The critical point $(0, 0)$ is a minimum of E_1 for $\omega > \omega_0(\varepsilon)$ and a saddle point of E_1 with two negative eigenvalues if $\omega < \omega_0(\varepsilon)$. The critical point $(a, 0)$ with $a > 0$ and $\omega > \omega_0(\varepsilon)$ related by equation (2.4) is a saddle point of E_1 with one negative and one zero eigenvalues. This conclusion agrees with the full bifurcation analysis of the GP equation (1.1) given in [11,25].

The zero eigenvalue for the asymmetric vortex with $a > 0$ is related to the rotational invariance of the vortex configuration, which can be placed at any $(\xi_0, \eta_0) = a(\cos\alpha, \sin\alpha)$ with arbitrary $\alpha \in [0, 2\pi]$. The corresponding eigenvector in the kernel of $E_1''(a, 0)$ is $R := [0, 1]^{\mathrm{T}}$.

(c) Stability of steadily rotating vortices

Stability of the two critical points of $E_1(\xi_0, \eta_0)$ is determined by equations of motion obtained from the leading-order Lagrangian

$$L_1(\xi_0, \eta_0) = \tfrac{1}{2}\varepsilon(\xi_0\dot{\eta}_0 - \dot{\xi}_0\eta_0) + E_1(\xi_0, \eta_0).$$

After dividing the Euler–Lagrange equations by ε, equations of motion take the form

$$\dot{\eta}_0 + \omega\xi_0(1 - \xi_0^2 - \eta_0^2) - \omega_0(\varepsilon)\xi_0 = 0$$

and

$$\dot{\xi}_0 - \omega\eta_0(1 - \xi_0^2 - \eta_0^2) + \omega_0(\varepsilon)\eta_0 = 0,$$

which can be written as the Hamiltonian system

$$\frac{\mathrm{d}}{\mathrm{d}t}\begin{bmatrix}\xi_0\\ \eta_0\end{bmatrix} = J\begin{bmatrix}\dfrac{\partial E_1}{\partial \xi_0}\\ \dfrac{\partial E_1}{\partial \eta_0}\end{bmatrix}, \quad J = \begin{bmatrix}0 & 1\\ -1 & 0\end{bmatrix}, \tag{2.8}$$

where E_1 in (2.7) serves as the Hamiltonian function.

Spectral stability of the two vortex solutions can be analysed from the linearization of the Hamiltonian system (2.8) at the critical point $(\xi_0, \eta_0) = (a, 0)$. Substituting $\xi_0 = a + \hat{\xi}_0\,\mathrm{e}^{\lambda t}$, $\eta_0 = \hat{\eta}_0\,\mathrm{e}^{\lambda t}$ and neglecting the quadratic terms in $(\hat{\xi}_0, \hat{\eta}_0)$ yield the spectral stability problem

$$\left.\begin{aligned}[\omega(1-3a^2) - \omega_0(\varepsilon)]\hat{\xi}_0 &= -\lambda\hat{\eta}_0\\ \text{and}\qquad [\omega(1-a^2) - \omega_0(\varepsilon)]\hat{\eta}_0 &= \lambda\hat{\xi}_0.\end{aligned}\right\} \tag{2.9}$$

For the symmetric vortex with $a = 0$, the spectral problem (2.9) admits a pair of purely imaginary eigenvalues with

$$\lambda^2 = -(\omega - \omega_0(\varepsilon))^2,$$

for both $\omega < \omega_0(\varepsilon)$ and $\omega > \omega_0(\varepsilon)$. For the asymmetric vortex with $a > 0$ and $\omega > \omega_0(\varepsilon)$ related by equation (2.4), the spectral problem (2.9) admits a double zero eigenvalue. These conclusions of the ODE theory agree with the numerical results obtained for the PDE model (1.1) in [11]. In particular, both the symmetric and asymmetric vortices were found to be spectrally stable for ω near $\omega_0(\varepsilon)$. The symmetric vortex was found to have a pair of purely imaginary eigenvalues near the origin coalescing at the origin for $\omega = \omega_0(\varepsilon)$. The asymmetric vortex was found to have an additional degeneracy of the zero eigenvalue due to the rotational symmetry.

The symmetric vortex with $a = 0$ is orbitally stable for $\omega > \omega_0(\varepsilon)$ because the critical point $(0, 0)$ is a minimum of E_1 for $\omega > \omega_0(\varepsilon)$. On the other hand, the asymmetric vortex is also orbitally stable because, although the critical point $(a, 0)$ is a saddle point of E_1, it is a constrained minimum of E_1 under the constraint eliminating the rotational symmetry and preserving the symplectic structure

of the Hamiltonian system (2.8). As $R = [0,1]^{\mathrm{T}}$ spans the kernel of the Hessian matrix $E_1''(a,0)$, the symplectic orthogonality constraint takes the form

$$\varphi := \begin{bmatrix} \xi_0 \\ \eta_0 \end{bmatrix} \in \mathbb{R}^2 : \quad \langle J^{-1}\varphi, R\rangle = 0, \tag{2.10}$$

which simplifies to $\xi_0 = 0$. The constraint $\xi_0 = 0$ removes the negative eigenvalue of the Hessian matrix $E_1''(a,0)$. Hence, the critical point $(a,0)$ is a constrained minimum of E_1 under the constraint (2.10) related to the rotational invariance.

3. Reduced energy for a pair of vortices of charge one

We now turn to the examination of a pair of vortices of charge one. It was argued in [18,19] that dynamics of two and more individual vortices can be modelled by using the reduced energy, which is given by the sum of energies of individual vortices and the interaction potential. In [16], a reduced energy for a pair of vortices of the opposite charge (vortex dipole) was obtained by using the same formal Rayleigh–Ritz method and analysis of resulting integrals in the limit $\varepsilon \to 0$.

Here, we rewrite the result of computations in Lemmas 3 and 4 in [16] in the case of a pair of vortices of the same charge one. We also add the nonlinear dependence of the frequency of vortex precession on the displacement a from the centre of the harmonic potential, which is modelled by the additional term in the kinetic energy (2.5).

Let the two vortices be located at the distinct points (x_1, y_1) and (x_2, y_2) on the plane such that $a_1 := (x_1^2 + y_1^2)^{1/2}$ and $a_2 := (x_2^2 + y_2^2)^{1/2}$ are small, ε is small, and $a := ((x_2 - x_1)^2 + (y_2 - y_1)^2)^{1/2}/\varepsilon$ is large. The two-vortex configuration has kinetic K and potential P energies given at the leading order by

$$K(x_1, x_2, y_1, y_2) = \frac{1}{2}\varepsilon \sum_{j=1}^{2} (x_j \dot{y}_j - y_j \dot{x}_j)\left[1 - \frac{1}{2}(x_j^2 + y_j^2)\right] \tag{3.1}$$

and

$$P(x_1, x_2, y_1, y_2) = \frac{1}{2}\varepsilon\omega_0(\varepsilon) \sum_{j=1}^{2} (x_j^2 + y_j^2) + \frac{1}{2}\varepsilon^2 \log[(x_1 - x_2)^2 + (y_1 - y_2)^2]. \tag{3.2}$$

In the reference frame rotating with the angular frequency ω, we can use the polar coordinates

$$x_j = \xi_j \cos(\omega t) - \eta_j \sin(\omega t) \quad \text{and} \quad y_j = \xi_j \sin(\omega t) + \eta_j \cos(\omega t), \quad j = 1, 2 \tag{3.3}$$

and rewrite the truncated kinetic and potential energies in the form

$$K(\xi_1, \xi_2, \eta_1, \eta_2) = \frac{1}{2}\varepsilon \sum_{j=1}^{2} (\xi_j \dot{\eta}_j - \dot{\xi}_j \eta_j) + \frac{1}{2}\varepsilon \sum_{j=1}^{2} \omega(\xi_j^2 + \eta_j^2)\left[1 - \frac{1}{2}(\xi_j^2 + \eta_j^2)\right]$$

and

$$P(\xi_1, \xi_2, \eta_1, \eta_2) = \frac{1}{2}\varepsilon\omega_0(\varepsilon) \sum_{j=1}^{2} (\xi_j^2 + \eta_j^2) + \frac{1}{2}\varepsilon^2 \log[(\xi_1 - \xi_2)^2 + (\eta_1 - \eta_2)^2],$$

where the nonlinear correction for the quadratic term $(\xi_j \dot{\eta}_j - \dot{\xi}_j \eta_j)$ in $K(\xi_1, \xi_2, \eta_1, \eta_2)$ is dropped to simplify the time evolution of the ODE system. In the remainder of this section, we obtain the existence and stability results for two vortices of charge one within the ODE theory.

(a) Existence of steadily rotating vortex pairs

Steadily rotating pairs of vortices are critical points of the action functional

$$E_2(\xi_1,\xi_2,\eta_1,\eta_2)=\frac{1}{2}\varepsilon\omega\sum_{j=1}^{2}(\xi_j^2+\eta_j^2)\left[1-\frac{1}{2}(\xi_j^2+\eta_j^2)\right]$$
$$-\frac{1}{2}\varepsilon\omega_0(\varepsilon)\sum_{j=1}^{2}(\xi_j^2+\eta_j^2)-\frac{1}{2}\varepsilon^2\log[(\xi_1-\xi_2)^2+(\eta_1-\eta_2)^2].$$

We assume that the two vortices are located along the straight line that passes through the centre of the harmonic potential. By using the rotational symmetry of the vortex configuration on the plane, we select the vortex location at two points $(\xi_1,\eta_1)=(b_1,0)$ and $(\xi_2,\eta_2)=(-b_2,0)$ for $b_1,b_2>0$. After dividing Euler–Lagrange equations for $E_2(b_1,-b_2,0,0)$ by ε, we obtain the following system of algebraic equations:

$$\left.\begin{aligned}&\omega b_1(1-b_1^2)-\omega_0(\varepsilon)b_1-\varepsilon(b_1+b_2)^{-1}=0\\ \text{and}\quad&\omega b_2(1-b_2^2)-\omega_0(\varepsilon)b_2-\varepsilon(b_1+b_2)^{-1}=0.\end{aligned}\right\}\tag{3.4}$$

Subtracting one equation from another, we obtain the constraint

$$(b_1-b_2)[\omega-\omega_0(\varepsilon)-\omega(b_1^2+b_1b_2+b_2^2)]=0.\tag{3.5}$$

The first root in (3.5) determines the symmetric vortex pair with $b_1=b_2=b$ related to ω by

$$\omega(b)=\frac{1}{1-b^2}\left[\omega_0(\varepsilon)+\frac{\varepsilon}{2b^2}\right].\tag{3.6}$$

The graph of $(0,1)\ni b\mapsto\omega\in\mathbb{R}$ has a global minimum at the point (b_*,ω_*), where

$$2\omega_*b_*^4=\varepsilon\ \ \Rightarrow\ \ \omega_*=\omega_0(\varepsilon)+\frac{\varepsilon}{b_*^2}>\omega_0(\varepsilon).\tag{3.7}$$

The second root in (3.5) determines the asymmetric vortex pair with $b_1\neq b_2$ related to ω by the system

$$\left.\begin{aligned}&\omega(1-b_1^2-b_1b_2-b_2^2)=\omega_0(\varepsilon)\\ \text{and}\quad&\omega b_1b_2(b_1+b_2)^2=\varepsilon,\end{aligned}\right\}\tag{3.8}$$

where the second equation was obtained from system (3.4) after dividing the first equation by b_1, the second equation by b_2 and subtracting the result. The branch of the asymmetric vortex pair bifurcates from the branch of the symmetric vortex pair at the point (b_{**},ω_{**}), where

$$4\omega_{**}b_{**}^4=\varepsilon\ \ \Rightarrow\ \ \omega_{**}=\omega_0(\varepsilon)+\frac{3\varepsilon}{4b_{**}^2}>\omega_0(\varepsilon).\tag{3.9}$$

As (b_*,ω_*) is the only (global) minimum of the graph of $(0,1)\ni b\mapsto\omega\in\mathbb{R}$ and (b_*,ω_*) is clearly different from (b_{**},ω_{**}), then we have $\omega_{**}>\omega_*$. Comparing (3.7) and (3.9), we obtain $3b_*^2>4b_{**}^2$ which yields $b_*>b_{**}$.

Figure 1 illustrates a typical example of the bifurcation diagram on the parameter plane (b,ω) for $\varepsilon=0.05$ with the notations used in (3.7) and (3.9). Both branches of the symmetric and asymmetric vortex pairs lie above the branch of a single vortex given by (2.4) with $a=b$.

It should be noted that the symmetry-breaking bifurcation from the symmetric to the asymmetric vortex pair was identified in the work of [4] (see also [6]). Here, we put this picture in the context of the stability and variational characterization of the two-vortex states.

(b) Variational characterization of vortex pairs

Extremal properties of the two critical points of $E_2(\xi_1,\xi_2,\eta_1,\eta_2)$ are studied from the Hessian matrix $E_2''(b_1,-b_2,0,0)$. This is a block-diagonal matrix in variables (ξ_1,ξ_2) and (η_1,η_2) with the

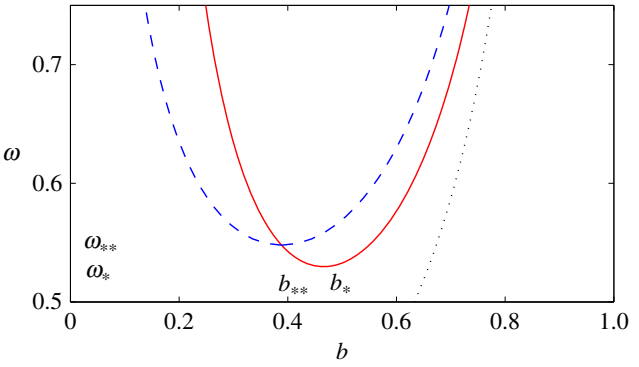

Figure 1. A typical example of the bifurcation diagram for two vortices of charge one, for $\epsilon = 0.05$. The symmetric (red, solid) and asymmetric (blue, dashed) pairs of vortices are shown on the parameter plane (b, ω). The branch of the single vortex displaced from the origin by the distance b is shown by a black dotted line. (Online version in colour.)

two blocks given by

$$L_+ := \partial_{\xi_i}\partial_{\xi_j} E_2(b_1, -b_2, 0, 0) = \varepsilon \begin{bmatrix} \omega(1-3b_1^2) - \omega_0(\varepsilon) + \dfrac{\varepsilon}{(b_1+b_2)^2} & -\dfrac{\varepsilon}{(b_1+b_2)^2} \\ -\dfrac{\varepsilon}{(b_1+b_2)^2} & \omega(1-3b_2^2) - \omega_0(\varepsilon) + \dfrac{\varepsilon}{(b_1+b_2)^2} \end{bmatrix} \tag{3.10}$$

and

$$L_- := \partial_{\eta_i}\partial_{\eta_j} E_2(b_1, -b_2, 0, 0) = \varepsilon \begin{bmatrix} \omega(1-b_1^2) - \omega_0(\varepsilon) - \dfrac{\varepsilon}{(b_1+b_2)^2} & \dfrac{\varepsilon}{(b_1+b_2)^2} \\ \dfrac{\varepsilon}{(b_1+b_2)^2} & \omega(1-b_2^2) - \omega_0(\varepsilon) - \dfrac{\varepsilon}{(b_1+b_2)^2} \end{bmatrix}. \tag{3.11}$$

Substituting the system (3.4) into L_- yields a simpler expression

$$L_- = \frac{\varepsilon^2}{b_1 b_2 (b_1+b_2)^2} \begin{bmatrix} b_2^2 & b_1 b_2 \\ b_1 b_2 & b_1^2 \end{bmatrix},$$

with a simple zero eigenvalue and a simple positive eigenvalue. The eigenvector for the zero eigenvalue of $E_2''(b_1, -b_2, 0, 0)$ is $R := [0, 0, b_1, -b_2]^{\mathrm{T}}$. This eigenvector is related to the rotational invariance of the vortex pair.

Eigenvalues of L_+ can be computed with some additional effort. For the symmetric vortex pair with $b_1 = b_2 = b$ and $\omega = \omega(b)$ given by (3.6), we simplify the entries of L_+ as follows:

$$L_+ = \varepsilon \begin{bmatrix} -2\omega(b)b^2 + \dfrac{3\varepsilon}{4b^2} & -\dfrac{\varepsilon}{4b^2} \\ -\dfrac{\varepsilon}{4b^2} & -2\omega(b)b^2 + \dfrac{3\varepsilon}{4b^2} \end{bmatrix}. \tag{3.12}$$

The two eigenvalues of L_+ are, thus, given by

$$\lambda_1 = -2\varepsilon\omega(b)b^2 + \frac{\varepsilon^2}{b^2} \quad \text{and} \quad \lambda_2 = -2\varepsilon\omega(b)b^2 + \frac{\varepsilon^2}{2b^2}. \tag{3.13}$$

Increasing b in the interval $(0, 1)$, we can detect two bifurcations at b_{**} and b_*, when the eigenvalues pass through the origin. For $b \in (0, b_{**})$, both eigenvalues of L_+ are positive. Hence,

the critical point $(b,-b,0,0)$ with the smallest displacement $b\in(0,b_{**})$ is a degenerate minimum of E_2 with a simple zero eigenvalue (due to L_-) for $\omega>\omega_{**}$. For $b\in(b_{**},b_*)$, we have $\lambda_2<0$ and $\lambda_1>0$, hence the critical point $(b,-b,0,0)$ with the smallest displacement $b\in(b_{**},b_*)$ is a saddle point of E_2 with one negative (λ_2) and one zero (due to L_-) eigenvalues for $\omega\in(\omega_*,\omega_{**})$. For $b\in(b_*,1)$, we have $\lambda_1<0$ and $\lambda_2<0$, hence the critical point $(b,-b,0,0)$ with the largest displacement $b\in(b_*,1)$ is a saddle point of E_2 with two negative (λ_1,λ_2) and one zero (due to L_-) eigenvalues for $\omega>\omega_*$.

For the asymmetric vortex pair with $b_1\neq b_2$, we use system (3.4) and simplify the entries of L_+ as follows:

$$L_+=\varepsilon\begin{bmatrix}-2\omega b_1^2+\dfrac{\varepsilon(2b_1+b_2)}{b_1(b_1+b_2)^2} & -\dfrac{\varepsilon}{(b_1+b_2)^2}\\ -\dfrac{\varepsilon}{(b_1+b_2)^2} & -2\omega b_2^2+\dfrac{\varepsilon(b_1+2b_2)}{b_2(b_1+b_2)^2}\end{bmatrix}.$$

Substituting the second equation of system (3.8) yields a simpler expression:

$$L_+=\frac{\varepsilon^2}{b_1b_2(b_1+b_2)^2}\begin{bmatrix}b_2^2+2b_1b_2-2b_1^2 & -b_1b_2\\ -b_1b_2 & b_1^2+2b_1b_2-2b_2^2\end{bmatrix},\tag{3.14}$$

with the determinant given by

$$\det(L_+)=-\frac{2\varepsilon^4}{b_1^2b_2^2(b_1+b_2)^4}[(b_1^2-b_2^2)^2+b_1b_2(b_1-b_2)^2].$$

As $\det(L_+)<0$, the matrix L_+ has one negative and one positive eigenvalue. Hence, the critical point $(b_1,-b_2,0,0)$ is a saddle point of E_2 with one negative (due to L_+) and one zero (due to L_-) eigenvalue for all $\omega>\omega_{**}$.

Let us now add the symplectic orthogonality constraint related to the symplectic matrix

$$J=\begin{bmatrix}0&0&1&0\\0&0&0&1\\-1&0&0&0\\0&-1&0&0\end{bmatrix},\tag{3.15}$$

which arises in the Hamiltonian system (3.19) below. As $R=[0,0,b_1,-b_2]^{\mathrm{T}}$ is the eigenvector for the zero eigenvalue of the Hessian matrix $E_2''(b_1,-b_2,0,0)$, the symplectic orthogonality constraint takes the form

$$\varphi:=\begin{bmatrix}\xi_1\\ \xi_2\\ \eta_1\\ \eta_2\end{bmatrix}\in\mathbb{R}^4:\quad\langle J^{-1}\varphi,R\rangle=0.\tag{3.16}$$

Owing to the structure of J and R, the constraint simplifies to the equation

$$b_1\eta_1-b_2\eta_2=0.\tag{3.17}$$

For the symmetric vortex pair with $b_1=b_2=b$, the constraint (3.17) is equivalent to $\eta_1=\eta_2$. Projecting L_+ in (3.12) to the subspace satisfying this constraint yields

$$\frac{1}{2}[1,1]\,L_+\begin{bmatrix}1\\1\end{bmatrix}=-2\varepsilon\omega(b)b^2+\frac{\varepsilon^2}{2b^2}=\lambda_2,$$

where λ_2 is defined by (3.13). As $\lambda_2>0$ for $b<b_{**}$ and $\lambda_2<0$ for $b>b_{**}$, the critical point $(b,-b,0,0)$ is a minimum of E_2 for $b\in(0,b_{**})$ and a saddle point of E_2 for $b\in(b_{**},1)$ under the constraint (3.16). No change in the number of negative eigenvalues of L_+ constrained by (3.16) occurs at $b=b_*>b_{**}$.

For the asymmetric vortex pair with $b_1 \neq b_2$, projecting L_+ in (3.14) to the subspace satisfying the constraint (3.16) yields

$$\frac{1}{b_1^2+b_2^2}[b_2,b_1]L_+\begin{bmatrix}b_2\\b_1\end{bmatrix}=\frac{\varepsilon^2}{b_1b_2(b_1+b_2)^2(b_1^2+b_2^2)}[(b_1^2-b_2^2)^2+2b_1b_2(b_1-b_2)^2]>0.$$

As the operator L_+ constrained by (3.16) is positive, the critical point $(b_1,-b_2,0,0)$ is a constrained minimum of E_2 under the constraint (3.16) for all $\omega>\omega_{**}$.

(c) Stability of vortex pairs

Stability of the two critical points of $E_2(\xi_1,\xi_2,\eta_1,\eta_2)$ is determined by equations of motion obtained from the leading-order Lagrangian

$$L_2(\xi_1,\eta_1,\xi_2,\eta_2)=\frac{1}{2}\varepsilon\sum_{j=1}^{2}(\xi_j\dot{\eta}_j-\eta_j\dot{\xi}_j)+E_2(\xi_1,\eta_1,\xi_2,\eta_2). \tag{3.18}$$

After dividing Euler–Lagrange equations by ε, equations of motion take the form

$$\dot{\eta}_1+\omega\xi_1(1-\xi_1^2-\eta_1^2)-\omega_0(\varepsilon)\xi_1-\frac{\varepsilon(\xi_1-\xi_2)}{(\xi_1-\xi_2)^2+(\eta_1-\eta_2)^2}=0,$$

$$\dot{\eta}_2+\omega\xi_2(1-\xi_2^2-\eta_2^2)-\omega_0(\varepsilon)\xi_2+\frac{\varepsilon(\xi_1-\xi_2)}{(\xi_1-\xi_2)^2+(\eta_1-\eta_2)^2}=0,$$

$$\dot{\xi}_1-\omega\eta_1(1-\xi_1^2-\eta_1^2)+\omega_0(\varepsilon)\eta_1+\frac{\varepsilon(\eta_1-\eta_2)}{(\xi_1-\xi_2)^2+(\eta_1-\eta_2)^2}=0$$

and

$$\dot{\xi}_2-\omega\eta_2(1-\xi_2^2-\eta_2^2)+\omega_0(\varepsilon)\eta_2-\frac{\varepsilon(\eta_1-\eta_2)}{(\xi_1-\xi_2)^2+(\eta_1-\eta_2)^2}=0,$$

which can be written as the Hamiltonian system

$$\frac{\mathrm{d}}{\mathrm{d}t}\begin{bmatrix}\xi_1\\\xi_2\\\eta_1\\\eta_2\end{bmatrix}=J\begin{bmatrix}\dfrac{\partial E_2}{\partial\xi_1}\\[2mm]\dfrac{\partial E_2}{\partial\xi_2}\\[2mm]\dfrac{\partial E_2}{\partial\eta_1}\\[2mm]\dfrac{\partial E_2}{\partial\eta_2}\end{bmatrix}, \tag{3.19}$$

where E_2 serves as the Hamiltonian function and J is defined by (3.15).

Linearizing equations of motion at the critical point $(\xi_1,\xi_2,\eta_1,\eta_2)=(b_1,-b_2,0,0)$ with

$$\xi_1=b_1+\hat{\xi}_1\,\mathrm{e}^{\lambda t},\quad \xi_2=-b_2+\hat{\xi}_2\,\mathrm{e}^{\lambda t},\quad \eta_1=\hat{\eta}_1\,\mathrm{e}^{\lambda t}\quad\text{and}\quad \eta_2=\hat{\eta}_2\,\mathrm{e}^{\lambda t},$$

yields the spectral stability problem

$$L_+\hat{\xi}=-\lambda\hat{\eta}\quad\text{and}\quad L_-\hat{\eta}=\lambda\hat{\xi}, \tag{3.20}$$

where $\hat{\xi}=[\hat{\xi}_1,\hat{\xi}_2]^{\mathrm{T}}$, $\hat{\eta}=[\hat{\eta}_1,\hat{\eta}_2]^{\mathrm{T}}$, whereas L_+ and L_- are given by (3.10) and (3.11).

For the symmetric vortex pair with $b_1=b_2=b$, the spectral stability problem (3.20) can be block-diagonalized into two decoupled problems:

$$\left.\begin{aligned}&\left[-2\omega(b)b^2+\frac{\varepsilon}{2b^2}\right](\hat{\xi}_1+\hat{\xi}_2)=-\lambda(\hat{\eta}_1+\hat{\eta}_2),\\&\frac{\varepsilon}{2b^2}(\hat{\eta}_1+\hat{\eta}_2)=\lambda(\hat{\xi}_1+\hat{\xi}_2)\end{aligned}\right\} \tag{3.21}$$

and

$$\left.\begin{aligned}\left[-2\omega(b)b^2+\frac{\varepsilon}{b^2}\right](\hat{\xi}_1-\hat{\xi}_2)&=-\lambda(\hat{\eta}_1-\hat{\eta}_2),\\ 0&=\lambda(\hat{\xi}_1-\hat{\xi}_2).\end{aligned}\right\} \tag{3.22}$$

The second block (3.22) yields a double zero eigenvalue with a non-diagonal Jordan block. The double zero eigenvalue is related to the rotational invariance of the symmetric vortex pair. The first block (3.21) yields a symmetric pair of eigenvalues from the characteristic equation

$$\lambda^2=\frac{\varepsilon}{2b^2}\left[2\omega(b)b^2-\frac{\varepsilon}{2b^2}\right]=-\frac{1}{2b^2}\lambda_2,$$

where λ_2 is defined by (3.13). As $\lambda_2>0$ for $b<b_{**}$ and $\lambda_2<0$ for $b>b_{**}$, we have $\lambda^2<0$ for $b<b_{**}$ and $\lambda^2>0$ for $b>b_{**}$. Hence, the symmetric vortex pair is stable for $b\in(0,b_{**})$ and unstable for $b\in(b_{**},1)$ with exactly one pair of real eigenvalues. This agrees with the variational characterization of the critical point $(b,-b,0,0)$, which is a minimum of E_2 for $b\in(0,b_{**})$ and a constrained saddle point of E_2 for $b\in(b_{**},1)$ under the constraint (3.16).

For the asymmetric vortex pair with $b_1\neq b_2$, the spectral stability problem (3.20) has again a double zero eigenvalue with a non-diagonal Jordan block, thanks to the rotational invariance of the vortex pair. It remains to find the other pair of eigenvalues λ. To eliminate the translational invariance, let us assume that $b_2\hat{\eta}_1+b_1\hat{\eta}_2\neq 0$, then $[\hat{\xi},\hat{\eta}]^{\mathrm{T}}\nparallel R=[0,0,b_1,-b_2]^{\mathrm{T}}$. If this is the case, we find from the spectral problem (3.20) that

$$\lambda b_1\hat{\xi}_1=\lambda b_2\hat{\xi}_2=\frac{\varepsilon}{(b_1+b_2)^2}(b_2\hat{\eta}_1+b_1\hat{\eta}_2).$$

after which the symmetric pair of eigenvalues is determined by the characteristic equation

$$\lambda^2=-\frac{\varepsilon^2}{b_1^2b_2^2(b_1+b_2)^4}[(b_1^2-b_2^2)^2+2b_1b_2(b_1-b_2)^2].$$

As $\lambda^2<0$, the asymmetric vortex pair is stable for all $\omega>\omega_{**}$. This agrees with the variational characterization of the critical point $(b_1,-b_2,0,0)$, which is a constrained minimum of E_2 under the constraint (3.16).

4. Numerical results for the Gross–Pitaevskii equation

To complement the ODE theory, we present direct numerical simulations of the PDE model (1.1) for a small value of ε. We use a Newton–Krylov solver to identify the vortex equilibria (both symmetric and asymmetric ones) in the frame rotating with frequency ω. Once these waveforms are identified, the vortex centre position b is extracted and a point is displaced on the parameter plane (b,ω). Subsequently, a linearization of the PDE model is performed in this co-rotating frame and the dominant eigenvalues (including those potentially responsible for instability) are extracted. In what follows, we set $\varepsilon=0.05$.

Figure 2 shows numerically obtained branches of the two-vortex solutions on the parameter plane (b,ω) (figure 2*a*) and (b,L) (figure 2*b*), where $L=b_1^2+b_2^2$ is used to emphasize the supercritical character of the relevant pitchfork bifurcation, in agreement with the diagrams used in [6].

The branch of a symmetric pair of two vortices can be obtained only for $\omega>\omega_*$, where $\omega_*\approx 0.587$, in line with the theoretical prediction on figure 1. The resulting solutions can be found both with $b>b_*$ and with $b<b_*$. The numerical value $b_*\approx 0.522$ from the PDE model is close to the predicted value $b_*^{(\mathrm{th})}\approx 0.490$ from the ODE theory. Along the branch of symmetric two-vortex solutions with $b<b_*$, a second bifurcation point is identified at $\omega_{**}\approx 0.693$ and the pair of branches of asymmetric two-vortex solutions is obtained for $\omega>\omega_{**}$. The numerical value $b_{**}\approx 0.352$ is again comparable with the predicted value $b_{**}^{(\mathrm{th})}\approx 0.408$.

Although the ODE theory captures fully the qualitative traits of the bifurcation diagram of the PDE model, there are some quantitative differences in the bifurcation points. These differences

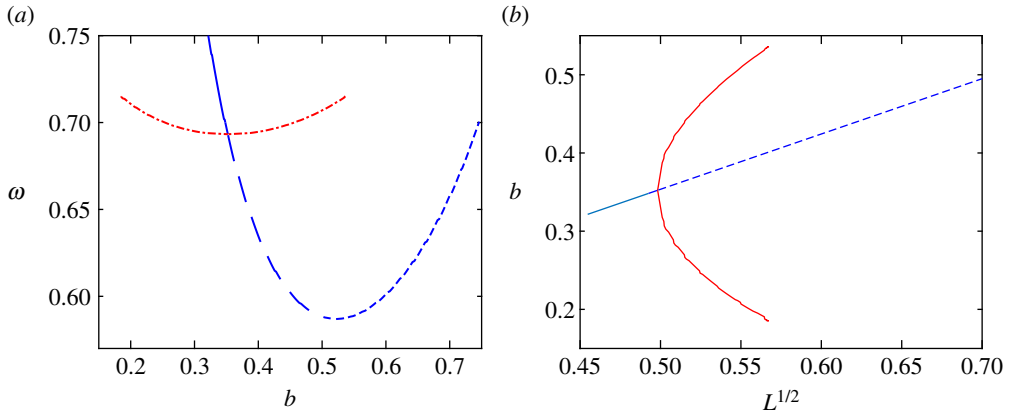

Figure 2. Bifurcation diagram of the symmetric and asymmetric vortex pairs for $\epsilon = 0.05$. (*a*) Branches of solutions on the parameter plane (b, ω). The solid line corresponds to the spectrally stable symmetric vortex pair, the dashed one corresponds to the unstable symmetric vortex pair, while the thick dash-dotted branch corresponds to the stable asymmetric vortex pair. (*b*) The bifurcation diagram in the variables (b, L) with $L = b_1^2 + b_2^2$. (Online version in colour.)

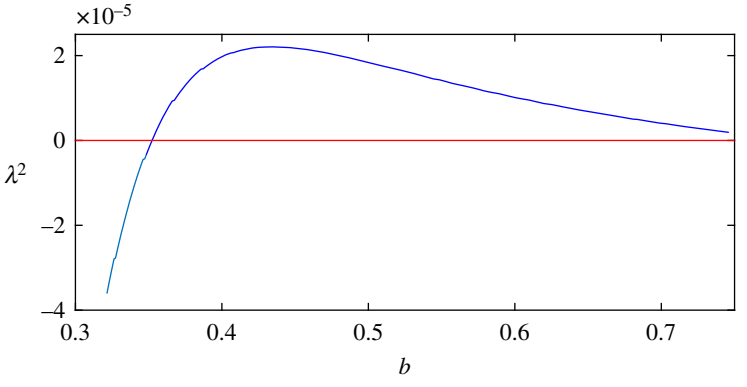

Figure 3. Squared eigenvalues of the spectral stability problem for the symmetric vortex pair. The unstable eigenvalue with $\lambda^2 > 0$ exists for $b > b_{**}$ in agreement with the ODE theory. (Online version in colour.)

exist, in part, because the ODE theory is valid in the semi-classical limit $\varepsilon \to 0$, whereas the PDE model is studied at a fixed finite value of ϵ. An additional key feature, however, is that the ODE theory assumes the inter-vortex interaction to be taking place over a uniform background. In the context of BECs, this is no longer the case, as the presence of the trap leads to a density modulation that screens the relevant interaction. Hence, quantitative deviations are expected from the theoretical prediction as a result of this screening effect. See [36] for a relevant discussion and the very recent work of [31] for a suggested modification of the equations of motion that accounts for this effect.

Figure 3 shows the squared eigenvalue of the spectral stability problem for the symmetric two-vortex solution. The dependence illustrates the destabilizing nature of the bifurcation at $\omega = \omega_{**}$ but not at $\omega = \omega_*$. Indeed, $\lambda^2 < 0$ for $b < b_{**}$ but $\lambda^2 > 0$ for both $b \in (b_{**}, b_*)$ and $b \in (b_*, 1)$, hence the symmetric two-vortex solution with $b > b_{**}$ is linearly unstable.

To manifest some typical profiles of the relevant configurations, in figure 4, we show two examples of the symmetric configuration for the same value of $\omega = 0.7$. This serves as a partial illustration of the 'folded' nature of the relevant branch of solutions, such that for each value of $\omega > \omega_*$, there exists a pair of symmetric two-vortex solutions (each of which is invariant under

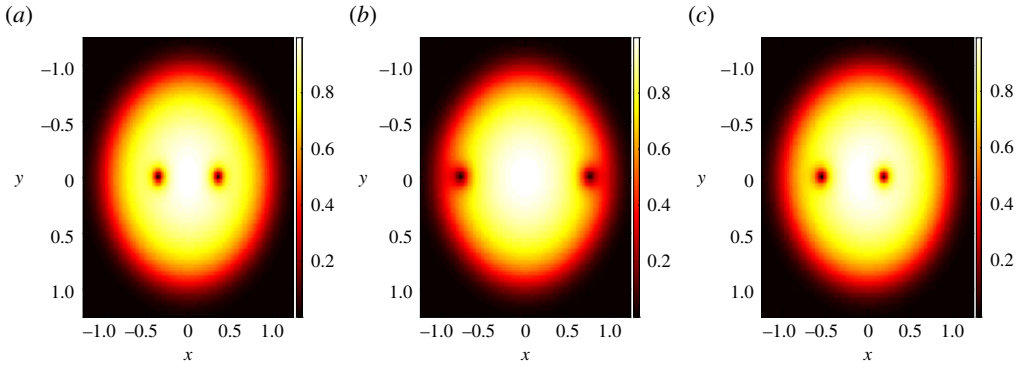

Figure 4. (*a*,*b*) Two examples of the symmetric vortex pair for the same value of $\omega = 0.7$. (*c*) An example of the asymmetric vortex pair for $\omega = 0.715$.

angular rotations). One of these (figure 4*a*) corresponds to the stable pair of vortices at a smaller-than-critical distance, while the other one (figure 4*b*) corresponds to the unstable pair of vortices at a larger-than-critical distance. In the latter case, the vortices are nearly at the edges of the cloud. Figure 4*c* illustrates an example of the stable asymmetric two-vortex solution for a value of $\omega = 0.715$.

5. Conclusion

We have revisited the existence and stability of two-vortex configurations in the context of rotating BECs. As a preamble to the ODE theory, we have discussed the existence and stability properties of a single vortex of charge one: the symmetric vortex is located at the centre of the trap and the asymmetric vortex is located at the periphery of the trap. We showed that the latter bifurcates at $\omega_1 = \omega_0(\varepsilon)$, where $\omega_0(\varepsilon)$ is the linear eigenfrequency of precession of a single vortex near the centre of the trap in the absence of rotation. The symmetric vortex is a local energy minimizer for $\omega > \omega_1$, whereas the asymmetric vortex is a constrained energy minimizer under the constraint eliminating rotational invariance.

We have also considered the relevant two-vortex configurations, when both vortices have the same charge one. In this context, the symmetric vortex pair bifurcates at $\omega_* > \omega_1$ via the saddle-node bifurcation of two different vortex pairs, whereas the asymmetric vortex pair bifurcates at $\omega_2 = \omega_{**} > \omega_*$ via the supercritical pitchfork bifurcation. The symmetric vortex pairs exist for $\omega > \omega_*$ and the two distinct solutions have either smaller-than-critical or larger-than-critical distance from the centre of the trap. The asymmetric vortex pairs exist for $\omega > \omega_{**}$ and bifurcate from the symmetric vortex pair with the smaller-than-critical distance from the centre of the trap. The two vortices in the asymmetric vortex pair are located at unequal distances from the trap centre. We showed that the symmetric vortex pair with the smaller-than-critical distance is a local energy minimizer for $\omega > \omega_2 = \omega_{**}$, whereas the asymmetric vortex pair is a constrained energy minimizer for $\omega > \omega_2$ under the constraint eliminating rotational invariance. We also showed that all other symmetric vortex pairs are unstable as they are saddle points of the energy under the same constraint. The ODE theory is compared with the full numerical approximations of the PDE model and a very good qualitative and reasonable quantitative correspondence is established between the two.

Data accessibility. This work has no experimental data.

Authors' contributions. P.G.K. contributed to numerical computations and D.E.P. contributed to analytical computations. Both the authors equally contributed to writing the paper.

Competing interests. The authors have no competing interests.

Funding. P.G.K. gratefully acknowledges support from NSF under grant no. PHY-1602994, and also from the Alexander von Humboldt Foundation as well as from the Stavros Niarchos Foundation under the Greek

Diaspora Fellowship Program. D.E.P. gratefully acknowledges the financial support from the state task of the Russian Federation in the sphere of scientific activity (Task no. 5.5176.2017/8.9).
Acknowledgements. The authors thank P. Bizon and C. Garcia–Azpeitia for discussions.

Appendix A. Derivation of the asymptotic expansion (2.5)

The kinetic energy $K(x_0, y_0)$ of a single vortex given by the asymptotic expansion (2.1) is determined in [16] from the expression

$$K = \frac{\mathrm{i}\varepsilon}{4\pi} \int_{\mathbb{R}^2} \eta_\varepsilon^2 (v\bar{v}_t - \bar{v}v_t)\,\mathrm{d}x,$$

where η_ε is the positive real radially symmetric ground state and v is represented by the free vortex solution of the defocusing nonlinear Schrödinger equation placed at the point (x_0, y_0). After substitution and separation of variables, the following expansion was obtained in the proof of Lemma 1 in [16]:

$$K = -\dot{x}_0 K_x - \dot{y}_0 K_y,$$

where

$$K_x = -\frac{\varepsilon^2}{2\pi} \int_{\mathbb{R}^2} \eta_\varepsilon^2(|x|) \frac{Y}{R^2}\,\mathrm{d}X\,\mathrm{d}Y + \mathcal{O}(\varepsilon^2|y_0|)$$

and

$$K_y = \frac{\varepsilon^2}{2\pi} \int_{\mathbb{R}^2} \eta_\varepsilon^2(|x|) \frac{X}{R^2}\,\mathrm{d}X\,\mathrm{d}Y + \mathcal{O}(\varepsilon^2|x_0|),$$

with $x = x_0 + \varepsilon X$, $y = y_0 + \varepsilon Y$ and $R = (X^2 + Y^2)^{1/2}$.

Here, we will extend the asymptotic expansion (2.1) in order to include the higher-order behaviour of $K(x_0, y_0)$ in (x_0, y_0) at the leading order in ε. By the symmetry of integrals, it is sufficient to analyse the leading order in the expression for K_x as a function of y_0 for $x_0 = 0$. Therefore, we define the leading-order part of K_x at $x_0 = 0$:

$$J(y_0) := -\frac{\varepsilon^2}{2\pi} \int_{\mathbb{R}^2} \eta_\varepsilon^2(r)\Big|_{r=\sqrt{\varepsilon^2X^2+(y_0+\varepsilon Y)^2}} \frac{Y}{R^2}\,\mathrm{d}X\,\mathrm{d}Y.$$

As J is smooth and $J(-y_0) = -J(y_0)$, we have $J(0) = J''(0) = J^{(4)}(0) = 0$. The first odd derivatives of J can be computed with the chain rule:

$$\begin{aligned} J'(0) &= -\frac{\varepsilon^2}{2\pi} \int_{\mathbb{R}^2} \partial_r \eta_\varepsilon^2(r)|_{r=\varepsilon R} \frac{Y^2}{R^3}\,\mathrm{d}X\,\mathrm{d}Y \\ &= -\frac{\varepsilon^2}{2\pi} \left[\int_0^\infty \partial_r \eta_\varepsilon^2(r)|_{r=\varepsilon R}\,\mathrm{d}R\right]\left[\int_0^{2\pi} \sin^2\theta\,\mathrm{d}\theta\right] \\ &= -\frac{\varepsilon}{2} \int_0^\infty \partial_r \eta_\varepsilon^2(r)\,\mathrm{d}r \\ &= \frac{\varepsilon}{2}\eta_\varepsilon(0)^2 \end{aligned}$$

and

$$\begin{aligned} J'''(0) &= -\frac{\varepsilon^2}{2\pi} \int_{\mathbb{R}^2} \left[\partial_r^3 \eta_\varepsilon^2(r)|_{r=\varepsilon R} \frac{Y^4}{R^5} + 3\partial_r^2 \eta_\varepsilon^2(r)|_{r=\varepsilon R} \frac{X^2Y^2}{\varepsilon R^6} - 3\partial_r \eta_\varepsilon^2(r)|_{r=\varepsilon R} \frac{X^2Y^2}{\varepsilon^2 R^7}\right] \mathrm{d}X\,\mathrm{d}Y \\ &= -\frac{3\varepsilon}{8} \int_0^\infty \left[\partial_r^3 \eta_\varepsilon^2(r) + \frac{1}{r}\partial_r^2 \eta_\varepsilon^2(r) - \frac{1}{r^2}\partial_r \eta_\varepsilon^2(r)\right] \mathrm{d}r \\ &= \frac{3\varepsilon}{8} \lim_{r\to 0} \left[\partial_r^2 \eta_\varepsilon(r)^2 + \frac{1}{r}\partial_r \eta_\varepsilon^2(r)\right]. \end{aligned}$$

Let us recall the approximation of the ground state η_ε in the Thomas–Fermi limit

$$\eta_0(x) := \lim_{\varepsilon\to 0} \eta_\varepsilon(x) = \begin{cases} (1-|x|^2)^{1/2}, & |x| \le 1, \\ 0, & |x| > 1, \end{cases}$$

which has been justified in [7,8]. By Proposition 2.1 in [8], for any compact subset K inside the unit disc, there is $C_K > 0$ such that

$$\|\eta_\varepsilon - \eta_0\|_{C^2(K)} \le C_K \varepsilon^2.$$

By using this bound, we compute $J'(0)$ and $J'''(0)$ as $\varepsilon \to 0$:

$$J'(0) = \frac{\varepsilon}{2}[1 + \mathcal{O}(\varepsilon^2)] \quad \text{and} \quad J'''(0) = -\frac{3\varepsilon}{2}[1 + \mathcal{O}(\varepsilon^2)],$$

from which we conclude that

$$J(y_0) = \tfrac{1}{2}\varepsilon y_0 \left[1 - \tfrac{1}{2}y_0^2 + \mathcal{O}(\varepsilon^2 + y_0^4)\right].$$

By the symmetry of K_x and similar computations for K_y, we obtain the expansion (2.5).

References

1. Pitaevskii LP, Stringari S. 2003 *Bose-Einstein condensation*. Oxford, UK: Oxford University Press.
2. Kevrekidis PG, Frantzeskakis DJ, Carretero-González R. 2015 *The defocusing nonlinear Schrödinger equation*. Philadelphia, PA: SIAM.
3. Fetter AL. 2009 Rotating trapped Bose-Einstein condensates. *Rev. Mod. Phys.* **81**, 647–691. (doi:10.1103/RevModPhys.81.647)
4. Navarro R, Carretero–González R, Torres PJ, Kevrekidis PG, Frantzeskakis DJ, Ray MW, Altuntas E, Hall DS. 2013 Dynamics of a few corotating vortices in Bose–Einstein condensates. *Phys. Rev. Lett.* **110**, 225301. (doi:10.1103/PhysRevLett.110.225301)
5. Castin Y, Dum R. 1999 Bose–Einstein condensates with vortices in rotating traps. *Eur. Phys. J. D* **7**, 399–412. (doi:10.1007/s100530050584)
6. Zampetaki AV, Carretero-González R, Kevrekidis PG, Diakonos FK, Frantzeskakis DJ. 2013 Exploring rigidly rotating vortex configurations and their bifurcations in atomic Bose-Einstein condensates. *Phys. Rev. E* **88**, 042914. (doi:10.1103/PhysRevE.88.042914)
7. Gallo C, Pelinovsky D. 2011 On the Thomas-Fermi ground state in a harmonic potential. *Asymptotic Anal.* **73**, 53–96.
8. Ignat R, Millot V. 2006 The critical velocity for vortex existence in a two-dimensional rotating Bose–Einstein condensate. *J. Funct. Anal.* **233**, 260–306. (doi:10.1016/j.jfa.2005.06.020)
9. Ignat R, Millot V. 2006 Energy expansion and vortex location for a two-dimensional rotating Bose–Einstein condensate. *Rev. Math. Phys.* **18**, 119–162. (doi:10.1142/S0129055X06002607)
10. Seiringer R. 2002 Gross-Pitaevskii theory of the rotating Bose gas. *Commun. Math. Phys.* **229**, 491–509. (doi:10.1007/s00220-002-0695-2)
11. Pelinovsky D, Kevrekidis PG. 2013 Bifurcations of asymmetric vortices in symmetric harmonic traps. *Appl. Math. Res. eXpress* **2013**, 127–164. (doi:10.1093/amrx/abs016)
12. Kollar R, Pego RL. 2012 Spectral stability of vortices in two-dimensional Bose–Einstein condensates via the Evans function and Krein signature. *Appl. Math. Res. eXpress* **2012**, 1–46. (doi:10.1093/amrx/abr007)
13. Kuopanportti P, Huhtamäki JAM, Möttönen M. 2011 Size and dynamics of vortex dipoles in dilute Bose-Einstein condensates. *Phys. Rev. A* **83**, 011603. (doi:10.1103/PhysRevA.83.011603)
14. Middelkamp S, Torres PJ, Kevrekidis PG, Frantzeskakis DJ, Carretero-Gonzalez R, Schmelcher P, Freilich DV, Hall DS. 2011 Guiding-center dynamics of vortex dipoles in Bose-Einstein condensates. *Phys. Rev. A* **84**, 011605. (doi:10.1103/PhysRevA.84.011605)
15. Möttönen M, Virtanen SMM, Isoshima T, Salomaa MM. 2005 Stationary vortex clusters in nonrotating Bose-Einstein condensates. *Phys. Rev. A* **71**, 033626. (doi:10.1103/PhysRevA.71.033626)
16. Pelinovsky D, Kevrekidis PG. 2011 Variational approximations of trapped vortices in the large-density limit. *Nonlinearity* **24**, 1271–1289. (doi:10.1088/0951-7715/24/4/013)

17. Torres PJ, Kevrekidis PG, Frantzeskakis DJ, Carretero-Gonzalez R, Schmelcher P, Hall DS. 2011 Dynamics of vortex dipoles in confined Bose-Einstein condensates. *Phys. Lett. A* **375**, 3044–3050. (doi:10.1016/j.physleta.2011.06.061)
18. Carretero-González R, Kevrekidis PG, Kolokolnikov T. 2016 Vortex nucleation in a dissipative variant of the nonlinear Schrödinger equation under rotation. *Phys. D* **317**, 1–14. (doi:10.1016/j.physd.2015.11.009)
19. Kolokolnikov T, Kevrekidis PG, Carretero–González R. 2014 A tale of two distributions: from few to many vortices in quasi-two-dimensional Bose-Einstein condensates. *Proc. R. Soc. Lond. Ser. A Math. Phys. Eng. Sci.* **470**, 20140048 (18 pp). (doi:10.1098/rspa.2014.0048)
20. Murray AV, Grosjek AJ, Kuopanportti P, Simula T. 2016 Hamiltonian dynamics of two same-sign point vortices. *Phys. Rev. A* **93**, 033649. (doi:10.1103/PhysRevA.93.033649)
21. Smirnov LA, Mironov VA. 2012 Dynamics of two-dimensional dark quasisolitons in a smoothly inhomogeneous Bose-Einstein condensate. *Phys. Rev. A* **85**, 053620. (doi:10.1103/PhysRevA.85.053620)
22. Kuznetsov EA, JuulRasmussen J. 1995 Instability of two-dimensional solitons and vortices in defocusing media. *Phys. Rev. E* **51**, 4479–4484. (doi:10.1103/PhysRevE.51.4479)
23. Kapitula T, Kevrekidis PG, Carretero–González R. 2007 Rotating matter waves in Bose–Einstein condensates. *Phys. D* **233**, 112–137. (doi:10.1016/j.physd.2007.06.012)
24. Contreras A, García-Azpeitia C. 2016 Global Bifurcation of Vortices and Dipoles in Bose-Einstein Condensates. *C. R. Math. Acad. Sci. Paris* **354**, 265–269. (doi:10.1016/j.crma.2015.11.011)
25. García-Azpeitia C, Pelinovsky DE. 2017 Bifurcations of multi-vortex configurations in rotating Bose-Einstein condensates. *Milan J. Math.* **85**, 331–367. (doi:10.1007/s00032-017-0275-8)
26. Germain P, Hani Z, Thomann L. 2016 On the continuous resonant equation for NLS. I. Deterministic analysis. *J. Math. Pures Appl.* **105**, 131–163. (doi:10.1016/j.matpur.2015.10.002)
27. Biasi A, Bizon P, Craps B, Evnin O. 2017 Exact lowest-Landau-level solutions for vortex precession in Bose-Einstein condensates. *Phys. Rev. A* **96**, 053615. (doi:10.1103/PhysRevA.96.053615)
28. Goodman RH, Kevrekidis PG, Carretero-González R. 2014 Dynamics of vortex dipoles in anisotropic Bose-Einstein condensates. *SIAM J. Appl. Dyn. Syst.* **14**, 699–729. (doi:10.1137/140992345)
29. Charalampidis EG, Kevrekidis PG, Farrell PE. 2018 Computing stationary solutions of the 2D Gross–Pitaevskii equation with deflated continuation. *Comm. Nonlinear Sci. Num. Simul.* **54**, 482–499. (doi:10.1016/j.cnsns.2017.05.024)
30. Danaila I, Protas B. 2017 Computation of ground states of the Gross-Pitaevskii functional via Riemannian optimization. (http://arxiv.org/abs/1703.07693)
31. Xie S, Kevrekidis PG, Kolokolnikov Th. 2017 Multi-vortex crystal lattices in Bose-Einstein condensates with a rotating trap. (http://arxiv.org/abs/1708.04336)
32. Wang W, Bisset RN, Ticknor C, Carretero-González R, Frantzeskakis DJ, Collins LA, Kevrekidis PG. 2017 Single and multiple vortex rings in three-dimensional Bose-Einstein condensates: existence, stability, and dynamics. *Phys. Rev. A* **95**, 043638. (doi:10.1103/PhysRevA.95.043638)
33. Bethuel F, Jerrard RL, Smets D. 2008 On the NLS dynamics for infinite energy vortex configurations on the plane. *Rev. Mat. Iberoam.* **24**, 671–702. (doi:10.4171/RMI/552)
34. Bethuel F, Saut J-C. 1999 Travelling waves for the Gross–Pitaevskii equation. *Ann. Inst. H. Poincare Phys. Theor.* **70**, 147–238.
35. Chiron D, Scheid C. 2017 Multiple branches of travelling waves for the Gross–Pitaevskii equation, hal-01525255.
36. McEndoo S, Busch Th. 2009 Small numbers of vortices in anisotropic traps. *Phys. Rev. A* **79**, 053616. (doi:10.1103/PhysRevA.79.053616)